Phenazineoxonium chloranilatomanganate and chloranilatoferrate: synthesis, structure, magnetic properties, and Mössbauer spectra

G. V. Shilov, Z. K. Nikitina, N. S. Ovanesyan, S. M. Aldoshin, and V. D. Makhaev*

Institute of Problems of Chemical Physics, Russian Academy of Sciences, 1 prosp. Akad. Semenova, 142432 Chernogolovka, Moscow Region, Russian Federation. Fax: +7 (496) 785 7048. E-mail: genshil@icp.ac.ru

Crystalline compounds $(H_3O)_2(phz)_3M_2(C_6O_4Cl_2)_3 \cdot (CH_3COCH_3)_n \cdot (H_2O)_n$ (n = 0—2, M = Mn (**1**), Fe (**3**)) were obtained in an acetone—water—tetrahydrofuran medium by the reaction of metal sulfates with chloranilic acid and phenazine (phz). The molecular and crystal structure of **1** was studied by X-ray diffraction at 300, 200, and 150 K. The crystal structure is composed of polymeric cationic $[(H_3O)_2(phz)_3]_n^{2n+}$ and anionic $[Mn_2(C_6O_4Cl_2)_3]_n^{2n-}$ layers having honeycomb structure and stacked in such a way that open-ended through-going channels accommodating H_2O and CH_3COCH_3 solvent molecules are formed; the H_3O^+ cations in the crystal structure are disordered. Magnetic studies indicate antiferromagnetic coupling of Mn^{2+} ions through chloranilate ligands; transition to a magnetically ordered state occurs at $T = 5$ K. According to powder X-ray diffraction data, complex **3** is isostructural with compound **1** but differs crucially from **1** in the electronic structure. According to Fe^{57} Mössbauer spectroscopy, complex **3** exists in delocalized mixed-valence Fe^{2+}/Fe^{3+} state and, as a consequence, shows ferromagnetic character of magnetic correlations and semiconductor type of electrical conductivity. These features were ascribed to the valence tautomerism $Fe^{2+} + (C_6O_4Cl_2)^{2-} \rightarrow Fe^{3+} + (C_6O_4Cl_2)^{\cdot 3-}$, which was observed for the first time for iron in a honeycomb structure.

Key words: manganese, iron, phenazineoxonium, chloranilate, non-innocent ligands, coordination polymer, valence tautomerism, molecular magnet, ferromagnetism, antiferromagnetism, Mössbauer spectroscopy.

In the last two decades, works on the design and investigation of high-dimensional multispin systems capable of cooperative magnetic ordering have been actively carried out.[1] Among these, coordination compounds with the oxalate ion as the ligand have been extensively studied. Owing to the polydentate behavior of the bis-chelate doubly charged $C_2O_4^{2-}$ anion toward metal ions, diverse coordination compounds involving this anion have been designed, in particular, magnetic metal oxalate networks of different dimensionality: chain structures of transition metal ions, layered compounds with a honeycomb motif, and three-dimensional cage complexes.[2—10] A number of bifunctional compounds have been synthesized whose crystal structures consist of ferromagnetic metal oxalate layers and organic cations that are located between the layers and exhibit nonlinear optical properties,[11] electrical conductivity,[12] optical activity,[13] or photochromism.[14]

Together with the study of oxalate complexes, the search for analogous magnetic compounds with other bis-chelate ligands has been in progress. The known bridging ligands such as 2,5-dihydroxy-1,4-benzoquinone and its derivatives with substituents in positions 3 and 6, *e.g.*, Cl, Br, NO_2, CN, CH_3, *etc.* could not but attract attention of researchers. All of these are strong dibasic acids and their anions contain two chelating units needed to form polymeric complexes with metals. Chloranilic acid ($H_2C_6O_4Cl_2$) is a rather common analytical reagent and it was studied most extensively. A series of complexes in which the chloranilate ion forms a bis-chelate bridge between two transition metal ions, Ni and Cu,[15] Mn,[16] Cu,[17] Co and Fe^{2+},[18] were obtained and exhaustively characterized. Several analogous compounds where the 2,5-dihydroxy-1,4-benzoquinone anion serves as the bis-chelate bridge between manganese, iron, and nickel ions were prepared.[19]

About two dozens of coordination compounds of divalent metals composed of infinite straight or zigzag-like metal chloranilate chains are currently known.[20—27] Thus it was shown that in the crystal structure of $\{[M^{II}(C_6O_4Cl_2)(H_2O)_2] \cdot 2H_2O\}_n$ (M = Mn, Fe, Co, Cu, Zn, and Cd), the octahedral environment of the metal ion is formed by two water molecules located in the *cis* positions and four oxygen atoms of two different chloranilate anions giving infinite zigzag-like metal chloranilate chains. A number of publications[24—29] consider the characteristic features of reactions of chloranilic acid with transition

Published in Russian in *Izvestiya Akademii Nauk. Seriya Khimicheskaya,* No. 6, pp. 1183—1193, June, 2011.

1066-5285/11/6006-1209

metal salts in water-alcohol medium in the presence of aromatic nitrogen heterocycles: pyrazine, dimethylpyrazine, bis-pyrimidine, terpyridine, and phenazine, which have two, three, or four donor nitrogen atoms and, hence, they are potential bridging ligands able to combine metal chloranilate chains into networks through M—N coordination bonds. Copper, manganese, cobalt, and iron compounds, $[M(C_6O_4Cl_2)(L)]_n$ (L is pyrazine), were synthesized;[20,24,25] in their crystal structures, straight metal chloranilate chains are combined into planar rectangular networks by bridging pyrazine molecules.

The results of investigations of two manganese complexes, $\{[Mn(C_6O_4Cl_2)(L)_{0.5}(H_2O)]\cdot\{(H_2O)\cdot(C_2H_5OH)\}_n$ (L is bis-pyrimidine) and $[Mn(C_6O_4Cl_2)(L')]_n$ (L′ is terpyridine) have been reported.[26] The crystal structure of the former compound comprises layers as a honeycomb structure in which every hexagon contains six Mn^{2+} ions, four $C_6O_4Cl_2^{2-}$ ions, and two neutral bis-pyrimidine ligands. The manganese ion occurs in an unusual seven-coordinate position consisting of two nitrogen atoms of the bis-pyrimidine molecule and five oxygen atoms of two $C_6O_4Cl_2^{2-}$ ions, and one water molecule. In the crystal structure of the latter compound, each Mn^{2+} ion also has an unusual seven-coordinate environment consisting of four oxygen atoms of two $C_6O_4Cl_2^{2-}$ ions and three nitrogen atoms of the terpyridine molecule. The chloranilate anions, which bridge the Mn^{2+} ions, form infinite zigzag-like metal chloranilate chains, which are combined into a three-dimensional crystal structure through stacking of the terpyridine ligands. Magnetic susceptibility measurements showed weak antiferromagnetic coupling of the neighboring Mn^{2+} ions. As shown previously,[21,27] dimethylpyrazine and phenazine are not coordinated to the metal (Cu, Fe, Co, Mn) in the aqueous medium, probably, due to steric hindrance created by α-substituents with respect to the donor nitrogen atoms. However, under the influence of these nitrogen heterocycles, instead of the zigzag-like chains, straight metal chloranilate chains hydrogen-bonded to give $\{[M(C_6O_4Cl_2)(H_2O)_2]L\}_n$ layers are formed (L is phenazine or dimethylpyrazine). The L molecules are arranged between the layers being held by the hydrogen bonds between nitrogen atoms and metal-coordinated water molecules. In the crystals of Fe, Co, and Mn complexes, there are weak antiferromagnetic intrachain exchange interactions.

Radically different results concerning the M^{2+}—chloranilate—phenazine systems were reported in the work[30] describing the synthesis and studies of the single crystals of four isostructural compounds, $\{[(H_3O)_2(phz)_3][M_2(C_6O_4Cl_2)_3]\cdot 2CH_3COCH_3\cdot 2H_2O\}_n$ (M = Cu, Co, Zn, and Cd, phz is phenazine). The crystal structure of the product with M = Cu was determined in detail. It was found that the compound is composed of the polymeric cationic layer $[(H_3O)_2(phz)_3]_n^{2n+}$ and the anionic layer $[M_2(C_6O_4Cl_2)_3]_n^{2n-}$, which have a honeycomb structure and are arranged above one another to form through-going channels, which accommodate H_2O and CH_3COCH_3 solvent molecules.

There are data concerning the synthesis of compounds whose crystal structures comprise neutral homometallic chloranilate honeycomb networks. These networks involve triply charged rare earth elements, $Pr_2(C_6O_4Cl_2)_3\cdot 8EtOH$ (see Ref. 31) and $Ln_2(C_6O_4Cl_2)_3\cdot nH_2O$ (Ln = Sc, Y, La, Ce, Pr, Nd, Gd, Tb, Yb, Lu);[32] for Ce, Pr, Nd, and Tb, $n = 18$; for Y, Gd, and Eu, $n = 16$.

Our studies of transition metal chloranilates were started with the attempts to synthesize the analogs of bimetallic network oxalates. A preliminary communication was published previously.[33] In nonaqueous reaction medium, we prepared amorphous compounds with the $[M^{II}Fe^{III}(C_6O_4Cl_2)_3]^-$ anions (M = Mn, Co, Ni, Cu) and Bu_4N^+ or Ph_4P^+ as the counter-ions. The obtained bimetallic complexes are X-ray amorphous; they are insoluble in water or organic solvents. Their IR spectra show the presence of only bridging chloranilate ligands. The Mössbauer spectroscopy and magnetic measurement data attest to transition of the complexes into a magnetically ordered state: the antiferromagnetic state for M^{II} = Mn ($T_N = 10$ K) and the ferrimagnetic state for M^{II} = Co, Ni, Cu ($T_C \leq 2$ K).[34] These data leave little doubt that the obtained compounds are network bimetallic chloranilate polymers, analogs of known oxalates.[3—5,7,9]

The latter fact, together with the proven existence of homometallic chloranilate honeycomb network structures,[28,29] stimulated us to analyze the controversial data on the products of reactions of metal chloranilates and phenazine[21,27—30] and to attempt to obtain the crystals of polymeric homometallic manganese or iron anionic chloranilate complexes with complex phenazine-hydroxonium cations using a previously described procedure.[30]

Experimental

The manganese complex $\{(H_3O)_2(phz)_3Mn_2(C_6O_4Cl_2)_3\cdot 2CH_3COCH_3\cdot 2H_2O\}_n$ (**1**) (including crystals suitable for X-ray diffraction) was prepared by a procedure similar to that for $\{(H_3O)_2(phz)_3Cu_2(C_6O_4Cl_2)_3\cdot 2CH_3COCH_3\cdot 2H_2O\}_n$ (**2**).[30] The macroscopic properties were studied for polycrystalline complexes **1** and $(H_3O)_2(phz)_3Fe_2(C_6O_4Cl_2)_3(CH_3COCH_3)_n(H_2O)_n$ (**3**), which were synthesized as follows. A solution of phenazine (0.6 mmol) in THF (~0.3 mmol mL^{-1}) and a solution of chloranilic acid (0.6 mmol) in acetone (~0.15 mmol mL^{-1}) were added with vigorous stirring to a solution of $Mn(ClO_4)_2$ or $Fe(ClO_4)_2$ (0.4 mmol) in water (~0.04 mmol mL^{-1}). After stirring for 30 min, the light, black-colored precipitate was filtered off, washed with acetone on the filter (3×3 mL), and dried *in vacuo* for 1 h at ~20 °C. The weight of the product was 0.28 g, which nearly corresponded to the quantitative yield (0.29 g).

Complex 1. Found (%): C, 50.10; H, 3.00; Cl, 14.93; Mn, 7.4; N, 5.92. $C_{60}H_{46}Cl_6Mn_2N_6O_{18}$. Calculated (%): C, 49.28; H, 3.15; Cl, 14.56; Mn, 7.52; N, 5.75.

Complex 3. Found (%): C, 48.91; H, 2.55; Cl, 14.65; Fe, 7.8; N, 5.74. $C_{60}H_{46}Cl_6Fe_2N_6O_{18}$. Calculated (%): C, 49.23; H, 2.98; Cl, 14.54; Fe, 7.64; N, 5.74.

The IR spectra of complexes **1** and **3** contain a strong absorption band at ~1500 cm^{-1} for the bridging C—O bonds and do not contain a C=O band at ~1650 cm^{-1}.

The X-ray diffraction experiment was carried out on a P4 four-circle automated diffractometer (graphite monochromator, λ(Mo-Kα) = 0.71073 Å, θ/2θ-scan mode). Three experiments were carried out for compound **1** using a 0.1×0.1×0.15 mm crystal at temperatures of 300, 200, and 150 K. The unit cell parameters were determined and refined using 35 reflections found in the θ angle range from 7 to 15°. The structure was solved by direct methods. The positions and thermal parameters of nonhydrogen atoms were refined in the isotropic and then in the anisotropic approximation by the full-matrix least-squares method. The phenazine hydrogen atoms were positioned geometrically and refined as the riding model. The position of the oxonium hydrogen atom was identified from the difference Fourier map and refined isotropically with bond length constraints.

The difference Fourier maps showed weak electron density peaks, which were identified as atoms that compose the solvent molecules. We were unable to refine the occupancies of the solvent molecule positions; these were specified to be equal for acetone and water. Only atomic coordinates were refined, and for the acetone molecule, bond length constraints were applied. The inclusion of the solvent molecules in the refinement reduced R_1 by ~0.2 and reduced the residual electron density from 1.3 to 0.2 e $Å^{-3}$.

The crystal data and the refinement statistics are summarized in Table 1. All calculations were performed using the SHELXTL 6.14 program package.[35]

Powder X-ray diffraction studies of compounds **1** and **3** were performed on an ARLX´TRA powder X-ray diffractometer (Thermo Electron Corporation, Switzerland). As the initial values for the refinement, the unit cell parameters obtained for the single crystals of compound **1** were used. The powder X-ray diffraction pattern of complex **1** coincides with that calculated from the single-crystal data. The X-ray diffraction pattern of iron complex **3** indicates that it is isostructural with complex **1**.

The magnetic susceptibility measurements for polycrystalline samples of **1** and **3** were carried out on a Quantum Design MPMS-5XL SQUID magnetometer in the temperature range of 2—300 K at an external magnetic field of 0.1 T. The dependence of the magnetic susceptibility on the magnetic field strength was measured in the range H = 0—5 T at 2 K. The molar magnetic susceptibility (χ_m) was calculated taking into account the total diamagnetism of atoms equal to $-112 \cdot 10^{-6}$ cm^3 mol^{-1}. The effective magnetic moment was calculated by the relation $\mu_{eff} = (8\chi T)^{1/2}$.

The ^{57}Fe Mössbauer spectra of the polycrystalline sample of **3** were recorded on a standard electrodynamic type unit in a constant-acceleration mode (WissEl GMBH). The low-temperature measurements were done using a CF-506 helium flow cryostat (Oxford Instruments) and a ^{57}Co source in the rhodium matrix. The spectrometer was calibrated against the spectrum of a 1 μm-thick ^{57}Fe foil. The spectra were processed by the least-squares method with the assumption of the Lorentzian absorption line shape.

Results and Discussion

The compound $\{(H_3O)_2(phz)_3Mn_2(C_6O_4Cl_2)_3 \cdot 2CH_3COCH_3 \cdot 2H_2O\}_n$ (**1**) crystallizes in the trigonal system (space group P-31m). Its crystal and molecular structure generally coincide with those of the copper analog **2** (see Ref. 30) being composed of anionic and cationic layers alternating along the unit cell c axis. Selected interatomic distances and bond angles are summarized in Table 2.

The anionic layer representing a honeycomb network of Mn^{2+} and $C_6O_4Cl_2^{2-}$ ions is extended parallel to the crystallographic plane xy. The neighboring $Mn(C_6O_4Cl_2)_3$ groups in the layer have different chiralities. The Mn atom coordinates six O atoms of three chloranilate ligands

Table 1. Selected crystallographic data for compound **1** at T = 300(2), 200(2), and 150(2) K

Parameter	300(2) K	200(2) K	150(2) K
Crystal system	Trigonal	Trigonal	Trigonal
Space group	P-31m	P-31m	P-31m
a/Å	14.086(1)	14.076(2)	14.073(1)
c/Å	8.917(1)	8.818(2)	8.766(1)
V/Å^3	1532.2(2)	1513.1(4)	1503.5(2)
Z	1	1	1
d_{calc}/g cm^{-3}	1.584	1.604	1.614
μ/cm^{-1}	7.52	7.62	7.67
Scanning range/deg	2—25	2—25	2—25
Number of experimental/independent reflections (R_{int})	2334/958 (0.0713)	2317/940 (0.0583)	2201/933 (0.1540)
Number of reflections with $I > 2\sigma(I)$	543	594	609
Number of refined parameters	86	86	86
GOOF	1.007	1.024	1.073
R_1 for reflections with $I > 2\sigma(I)$	0.0566	0.0494	0.0486
wR_2 for all reflections	0.1791	0.1371	0.1540

Table 2. Selected bond lengths (*d*) and bond angles (ω) in the MnO_6 fragment of compound **1**

Bond length	*d*/Å	Angle	ω/deg
Mn(1)—O(1)	2.171(4)	O(1)—Mn(1)—O(1)*1	84.9(2)
Cl(1)—C(2)	1.760(8)	O(1)—Mn(1)—O(1)*2	100.0(1)
O(1)—C(1)	1.252(6)	O(1)—Mn(1)—O(1)*3	75.3(2)
C(1)—C(2)	1.390(6)	O(1)—Mn(1)—O(1)*4	173.8(2)
C(1)—C(1)*3	1.546(11)		
C(2)—C(1)*6	1.390(6)		

Note. Symmetry codes used to generate equivalent atoms: *1 $-y+1, -x+1, -z$; *2 $-x+y+1, -x+1, z$; *3 $x, x-y, -z$; *4 $-x+y+1, y, -z$.

(Fig. 1). Due to the position of the Mn atom in the crystal structure (at the intersection of the threefold and twofold axes), the three ligands are related by a threefold axis, each being formed by multiplication of its independent part by the twofold axis and the plane. As in isomorphous compound **2**, all metal—oxygen bonds in the MnO_6 octahedron are equal, amounting to 2.171(4) Å, but the angles noticeably differ from 90 and 180° (see Table 2). Since the lengths of same-type bonds and the angles in the structures determined at three temperatures coincide to within the experimental error, Table 2 presents only the data obtained at 300 K. The distortion of MnO_6 can be represented as two identical triangular MnO_3 pyramids compressed along the threefold axis and slightly rotated about this axis relative to each other.

The cationic layer $[(H_3O)_2(phz)_3]_n^{2+}$ is formed by the $(H_3O)^+$ oxonium ions and (phz) phenazine molecules through O...N hydrogen bonds (2.66 Å) and is also a network parallel to the *xy* plane. The O atom of the oxonium ion in structure **1** is located on the threefold axis but is shifted from the intersection point with the twofold axis and, hence, it is disordered over two positions, whereas in structure **2**, it is located at the intersection of the threefold and twofold axes. Thus, in structure **1**, the oxonium ion is arranged asymmetrically between the metal centers related by a translation along the *c* axis, its three H atoms are located on the twofold axes intersecting the threefold axis at this point, *i.e.*, the oxonium ion has a usual pyramidal structure. As regards the copper analog **2**, the planar structure was accepted for the oxonium ion with the O atom being located strictly in the midpoint between the Cu ions. The three oxonium H atoms are involved in strong O—H...N hydrogen bonds with three phenazine molecules: O...N, 2.66 Å; O—H, 0.90 Å; H...N, 1.72 Å; and O—H—N angle, 163.3° (Fig. 2).

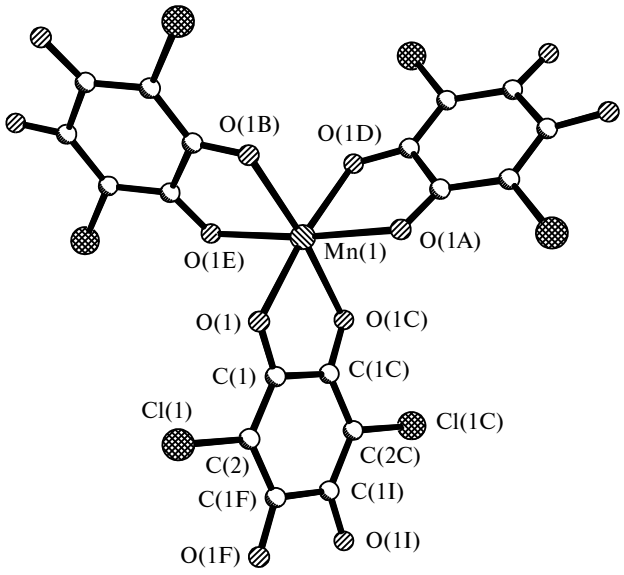

Fig. 1. Structural unit $Mn(C_6O_4Cl_2)_3$ in complex **1**.

Previously,[30] stacking interactions between the anionic and cationic layers were shown to exist in structure **2**, as the inclinations of the planes of the phenazine molecules in the cationic layer and the planes of the chloranilate ligands in the anionic layer are equal. A similar situation was also found for the crystal structure of compound **1**. Short distances (3.26 Å) occur between the planes of the chloranilate ligands and the corresponding phenazine molecules.

In structure **1**, barrel-like through-going channels ~8 Å in diameter run along the crystallographic direction *z* (Fig. 3). From the weak electron density peaks that were observed in the difference Fourier maps, we were able to reconstruct guest solvent molecules, acetone and water, in these channels. The guest molecules are located in the cavities of anionic and cationic layers near the symmetry elements $(-3)m$, hence, they are disordered. Figure 3 shows one of the arrangement patterns of the guest molecule. Due to the small size, the cavity cannot accommodate simultaneously two acetone molecules or an acetone or water molecule but can accommodate two water molecules. It was impossible to refine the site occupancies of water and acetone molecules; therefore, it was assumed that the numbers of cavities occupied by water and acetone molecules in the crystal structure are equal. Then two H_2O molecules and one CH_3COCH_3 molecule per formula unit are present. Meanwhile, chemical analysis data point to two H_2O and two CH_3COCH_3 molecules. Since we cannot determine precisely the numbers of water and acetone molecules from X-ray diffraction data, presumably, some of the guest molecules are disordered being located in the channels between the anionic and cationic layers.

As can be seen from Table 2, the four C—O bonds in the chloranilate anion are equivalent. This brings about the question of whether this bond length distribution may be a consequence of structure determination in space group $P\text{-}31m$. The dependence of the thermal vibration parameters of atoms on temperature implies the presence of

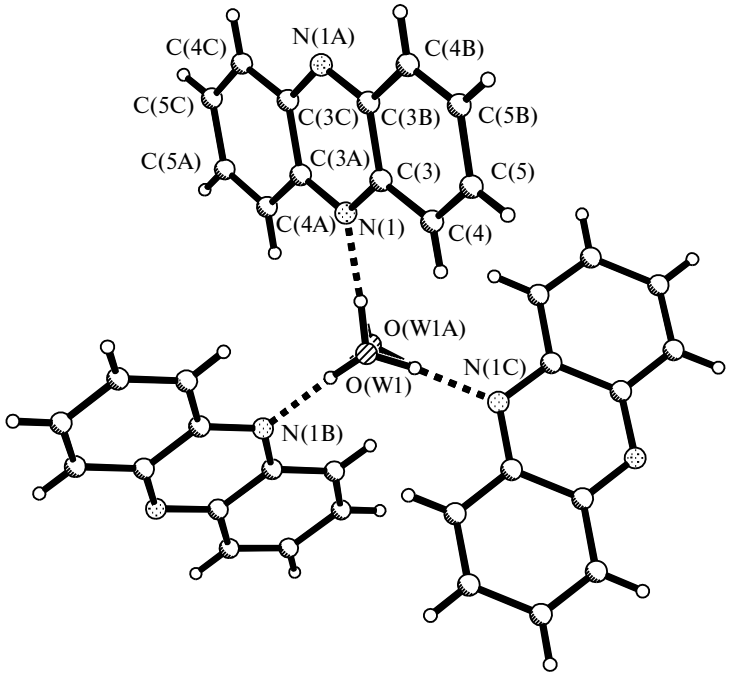

Fig. 2. Environment of the oxonium cation formed by phenazine molecules. The dashed lines show the hydrogen bonds.

a noticeable temperature-independent contribution in the thermal vibration amplitude, and this indicates that the crystal structure is most likely averaged over a number of states. It can be seen in Figure 4 that the static contribution to the average squared amplitude of thermal vibrations U^2 determined from X-ray diffraction data by ex-

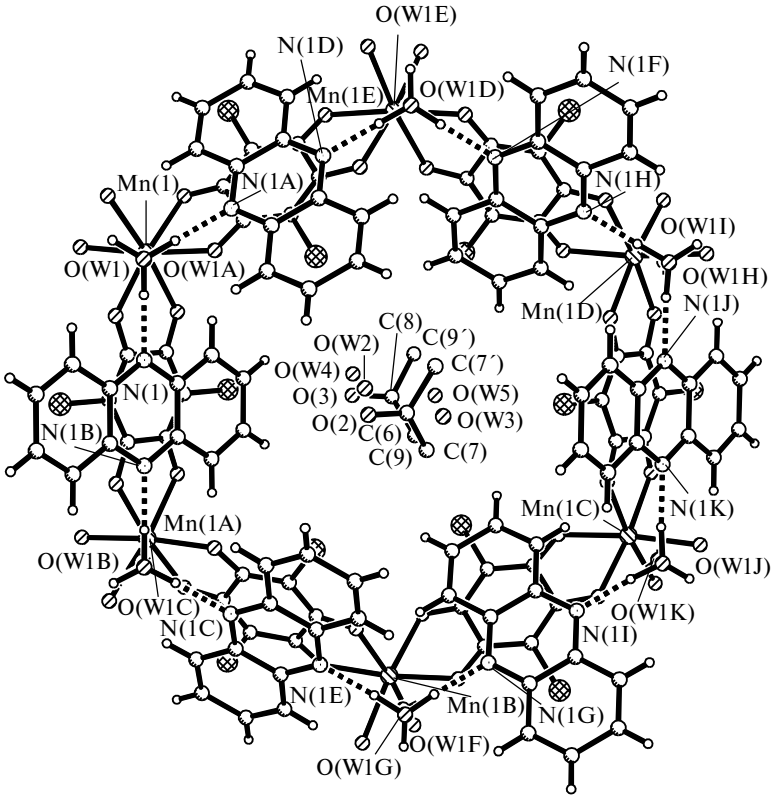

Fig. 3. Fragment of the projection of the anionic and cationic layers onto the crystallographic plane *xy*.

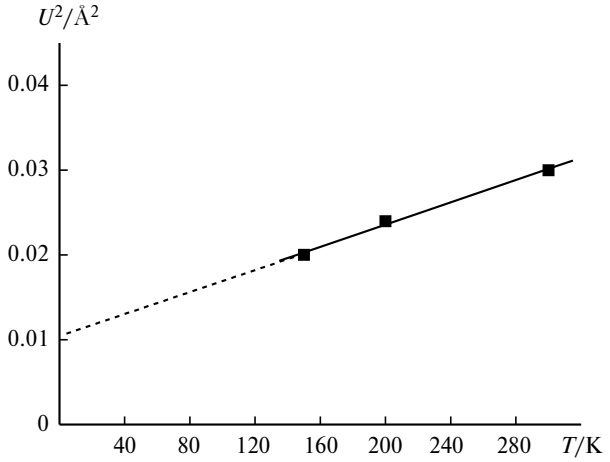

Fig. 4. Squared amplitude of thermal vibrations U^2 of O(1) along axis *b vs.* temperature.

trapolating the straight-line temperature dependence of U^2 to 0 K is 0.012 Å^2 (it should tend to zero without the static contribution), which is indicative of the presence of different states of the structure, in particular, of the anionic network.

The existence of different states may be due to the interaction of the chloranilate anions with the oxonium cations. Due to statistical disorder in the crystal structure, the oxonium ion may produce distortions in the metal chloranilate centers through the electrostatic interactions with them, the distortions being statistically distributed in the anionic network, and averaging of these distortions is responsible for the appearance of the temperature-independent static component to the rms deviations of atoms.

We attempted to remove the water and acetone solvent molecules from sample **1**. If the powdered complex **1** is kept for a long time in vacuum at gentle heating (30—40 °C), the mass loss corresponds to the removal of solvent molecules. However, as shown by X-ray diffraction studies, after long-term (>1 month) keeping of the crystal of **1** *in vacuo*, the water and acetone molecules still remain in the anionic and cationic layers. This was accompanied by a decrease in the unit cell parameter *c* (by 0.19 Å) and a decrease in the reflection intensities. Perhaps, some of the disordered solvent molecules located in the channels between the anionic and cationic layers are removed on evacuation, resulting in a decrease in the period *c* of the unit cell determined by X-ray diffraction. The decrease in the diffraction peak intensity may be attributed to partial destruction of the crystal upon removal of the guest molecules.

Compound **3** was not isolated as crystals. However, its powder X-ray diffraction patterns were identical to those of compound **1**, which indicates that the compounds are isostructural. According to powder X-ray diffraction data, structure **3** has the following unit cell parameters at T = 300 K: a = 13.698 Å, c = 9.312 Å, V = 1513.2 Å, Z = 1, space group P-31m. The Fe—O bond length (2.075 Å) and the chelate angle (μ = 78.6°) were calculated from the unit cell parameter a and the average size of the chloranilate anion with allowance for the fact that the distance between two neighboring metal atoms in the Fe—$C_6O_4Cl_2$—Fe unit is $a/\sqrt{-}3$ = 7.91 Å.

The charge and spin states of the iron ions in sample **3** were investigated by ^{57}Fe Mössbauer spectroscopy. According to the chemical composition of the compound, the expected charge of the iron ions is +2. In the octahedral oxygen coordination by chloranilate ions, this should correspond to the high-spin state (S = 2). For the localized Fe^{3+} and Fe^{2+} ions in the octahedral oxygen environment, the isomer shifts at room temperature are in the range of 0.36—0.40 and 1.10—1.20 mm s^{-1}, respectively. The iron Mössbauer spectrum of the complex (Table 3) measured at room temperature is manifested as two quadrupole doublets with parameters untypical of pure high-spin Fe^{2+} ($d\alpha^5d\beta$) or Fe^{3+} ($d\alpha^5$) states. The intermediate isomer shift values undoubtedly indicate that some of the iron ions in the compound have a charge of +3. The spectral parameters for 85 K were obtained by decomposition into three asymmetric quadrupole doublets with the assumption of equal areas of each constituent lines of the doublet. At room temperature, the spectrum is satisfactorily approximated by two symmetric doublets. The unusual temperature behavior of the Mössbauer parameters is attributable to the $Fe^{2+}Fe^{3+} \leftrightarrow Fe^{3+}Fe^{2+}$ electron exchange dynamics (see below). This situation is quite possible, as chloranilate is a so-called non-innocent ligand.[36] The close energy levels of iron(II) $d\pi$ orbitals and free chloranilate π orbitals enable the $d\beta$-electron transfer from the Fe^{2+} ion to the neighboring chloranilate dianion, $(C_6O_4Cl_2)^{2-}$ to give Fe^{3+} and the radical trianion $(C_6O_4Cl_2)^{\cdot 3-}$.[36] If the isomer shift of the Fe^{2+} and Fe^{3+} components is linearly related to the contribution of each ion involved in the exchange, Fe^{2+} and Fe^{3+}, then their ratio estimated from the data of Table 3 is 1 : 1 (the accuracy is not higher than 5%) and the composition of the compound can be written as $[(H_3O^+)_2(phz)_3][Fe^{2+}Fe^{3+}(C_6O_4Cl_2^{2-})_2(C_6O_4Cl_2^{\cdot 3-})] \cdot 2C_2H_6CO \cdot 2H_2O$.

The probable structure of the anionic layer of complex **3** corresponding to the structurally ordered charge distribution is shown in Fig. 5.

The temperature dependence of the effective magnetic moment of complex **1** is shown in Fig. 6. At 300 K, μ_{eff} = 8.17 μ_B, while as the temperature decreases (to 50 K), this value slowly decreases and then sharply drops. The calculated μ_{eff} value for two uncoupled spins of Mn^{2+} (S = 5/2) is 8.36 μ_B; apparently, this is attained at temperatures exceeding the limit of measurements. This behavior of the effective moment unambiguously attests to enhancement of antiferromagnetic Mn^{2+}—$(C_6O_4Cl_2)^{2-}$—Mn^{2+} correlations in the complex upon temperature decrease.

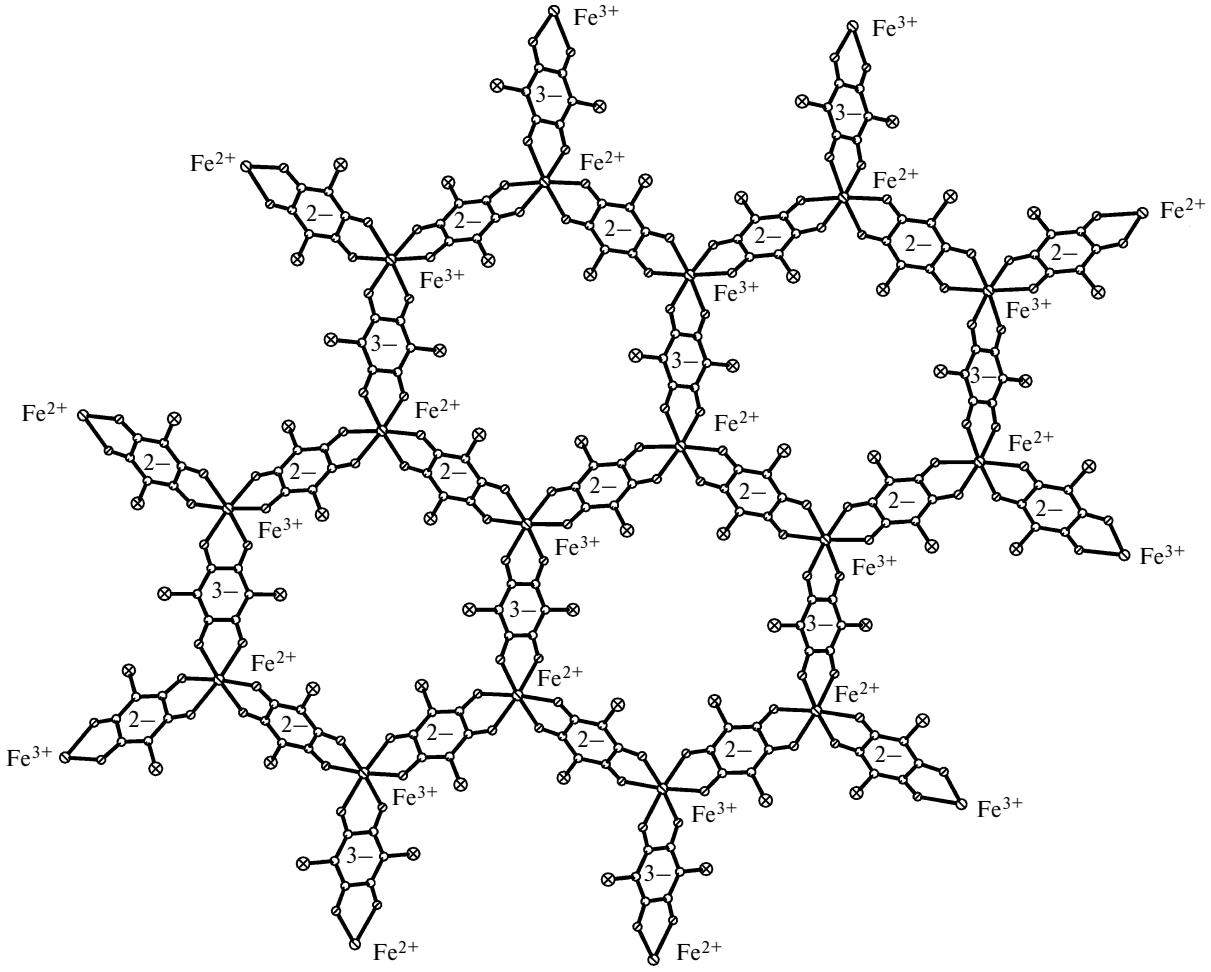

Fig. 5. Probable structure of the anionic layer of compound **3** at ordered charge distribution.

The temperature dependence of the inverse susceptibility is well described by the Curie—Weiss expression $\chi_m = C_M/(T - \theta)$ (Fig. 7). The negative Weiss constant ($\theta = -10.2$ K) found by the linear extrapolation of the dependence $\chi^{-1}(T)$ to the low-temperature region also attests to the antiferromagnetic coupling of Mn^{2+} ions through the $(C_6O_4Cl_2)^{2-}$ ligands. The magnitude and the sign of the Weiss constant imply the possibility of antiferromagnetic transition at temperatures below 10 K. Indeed, the temperature dependence of the magnetic sus-

Table 3. Mössbauer spectral parameters of compound **3**

T/K	State	δ*	ΔE_Q**	Γ_1***	Γ_2***	Fraction (%)
		mm s^{-1}				
295	Fe^{3+}	0.58	1.36	0.33	0.33	19
	$Fe^{2.5+}$	0.79	0.77	0.55	0.55	81
85	Fe^{3+}	0.51	1.29	0.75	0.57	37
	$Fe^{2.5+}$	0.72	1.45	0.60	0.59	28
	Fe^{2+}	1.10	1.42	0.27	0.50	34

* Isomer shift relative to α-Fe.
** Quadrupole splitting.
*** Line width.

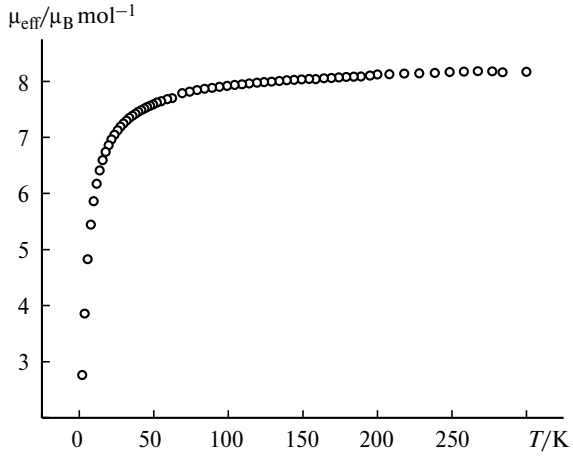

Fig. 6. Temperature dependence of the effective magnetic moment (μ_{eff}) of sample **1** ($H = 1$ kOe).

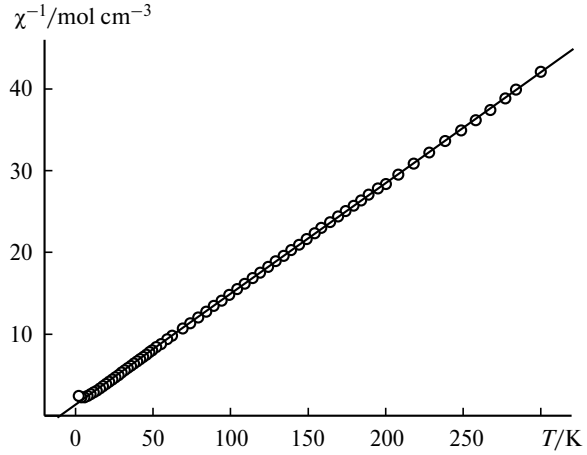

Fig. 7. Inverse magnetic susceptibility (χ^{-1}) of complex **1** *vs.* temperature ($H = 1$ kOe). The Curie—Weiss constant $\theta = 10.2$ K was found by linear extrapolation to lower temperatures.

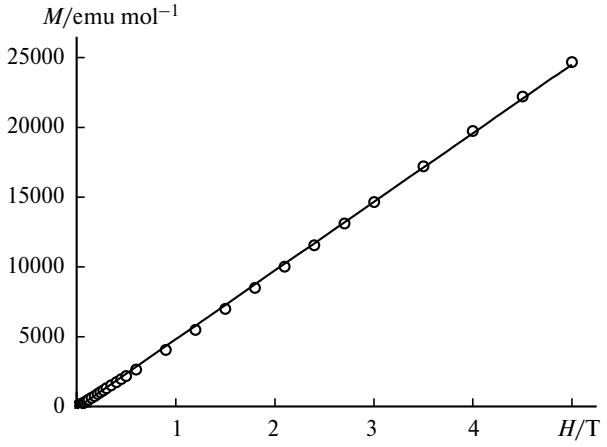

Fig. 9. Molar magnetic moment (M) of sample **1** *vs.* external magnetic field at 2 K.

ceptibility (Fig. 8) shows a maximum at $T = 5$ K, which is typical of a substance that undergoes a paramagnetic to antiferromagnetic transition.

The sample magnetization measured at 2 K shows a linear dependence on the applied magnetic field typical of an antiferromagnet (Fig. 9). In the absence of an external field, the total magnetic moment is zero.

In isomorphous copper compound **2** (see Ref. 30), no antiferromagnetic transition occurs down to 2 K. Probably, this is related to the weaker through-ligand exchange interaction of Cu^{II} centers. Indeed, the Curie—Weiss constant calculated from the experiment is −3.8 K, *i.e.*, it is three times lower than the value we found for Mn analog **1**.

In compound **3**, the temperature dependence of the effective moment follows the opposite trend as compared with the Mn analog: as the temperature decreases, the iron ion moments tend to parallel orientation, which is manifested as considerable increase in the effective magnetic moment (Fig. 10). For independent Fe^{2+} ions, the expected effective magnetic moment at $S = 2$ and $g = 2.2$ would be 7.6 μ_B per formula unit. Moreover, the $Fe^{2+}—(C_6O_4Cl_2)^{2-}—Fe^{2+}$ exchange interactions, as in the case of the isomorphous crystals with Mn^{2+} (**1**) and Cu^{2+} (**2**), are expected to be antiferromagnetic. Note that the increase in the effective moment is noticeable even at 300 K.

The temperature behavior of the inverse magnetic susceptibility of the sample is also unusual. The linear extrapolation of the dependence is possible only down to ~200 K (Fig. 11). The positive and rather high Curie—Weiss constant ($\theta = 40$ K) implies a high ferromagnetic transition temperature. However, below 200 K the magnetic moment deviates toward lower values, *i.e.*, a contribution of the competing antiferromagnetic coupling appears, apart from the ferromagnetic coupling (see Fig. 11).

The sharp increase in the magnetic susceptibility below ~18 K can be attributed to the onset of ferro- or ferri-

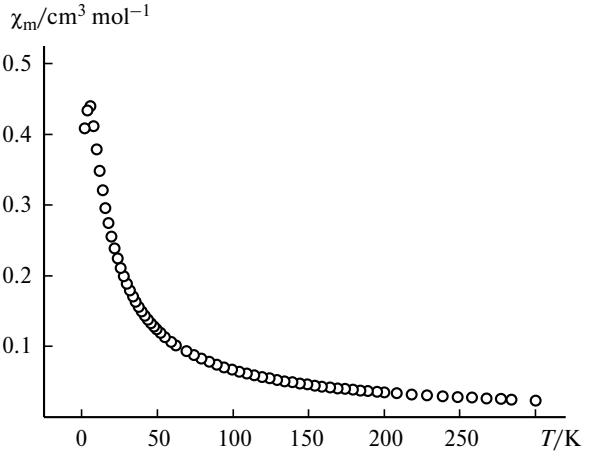

Fig. 8. Temperature dependence of the molar magnetic susceptibility (χ_m) of sample **1** at $H = 1$ kOe. The maximum at $T = 5$ K corresponds to the antiferromagnetic transition.

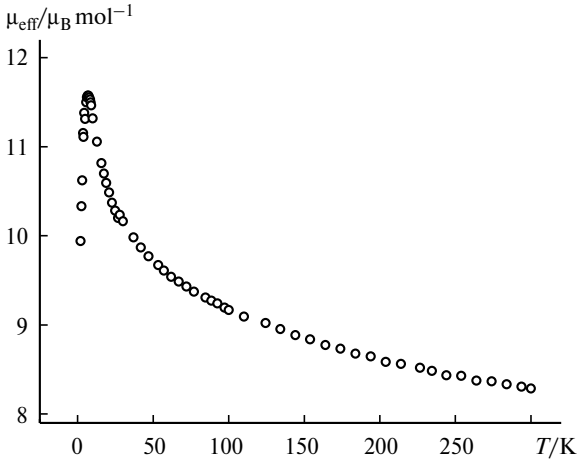

Fig. 10. Temperature dependence of the effective magnetic moment (μ_{eff}) for complex **3** in the external field $H = 100$ Oe.

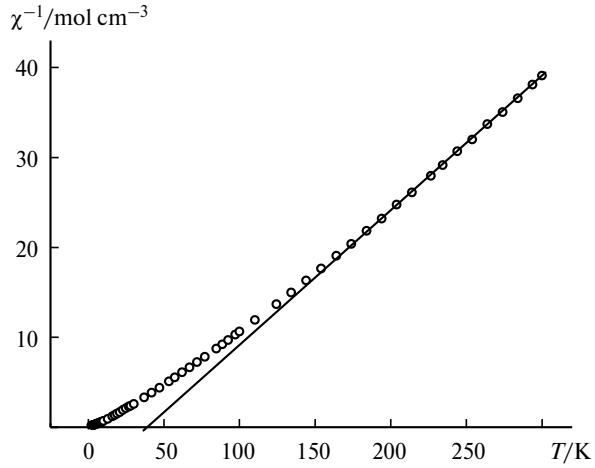

Fig. 11. Temperature dependence of the inverse magnetic susceptibility (χ^{-1}) of sample **3** measured in the external magnetic field H = 100 Oe. The Curie—Weiss constant θ = 40 K was found by linear extrapolation from higher temperature region.

magnetic transition (Fig. 12). It can be seen that two sample cooling modes, namely, zero-field cooling (ZFC) and field cooling (FC) at 0.1 T, result in magnetization values starting to deviate from each other at $T < 20$ K. Note that in the magnetically ordered state, field-cooled magnetization is normally much higher than zero-field-cooled magnetization due to the temperature-dependent constant of magnetocrystalline anisotropy.

The field dependence of magnetization for sample **3** at 2 K is typical of the paramagnetic state. The dependence is adequately described by the sum of two Brillouin functions with spins of 2 and 2.5 (Fig. 13). The magnetic moment per formula unit at a maximum external field strength of 5 T is 7.5 μ_B but still it is not saturated. Thus, contrary to the expected antiferromagnetic ordering, the opposite trend to ferromagnetic ordering of iron moments is observed, although the long-range magnetic order is not established down to 2 K.

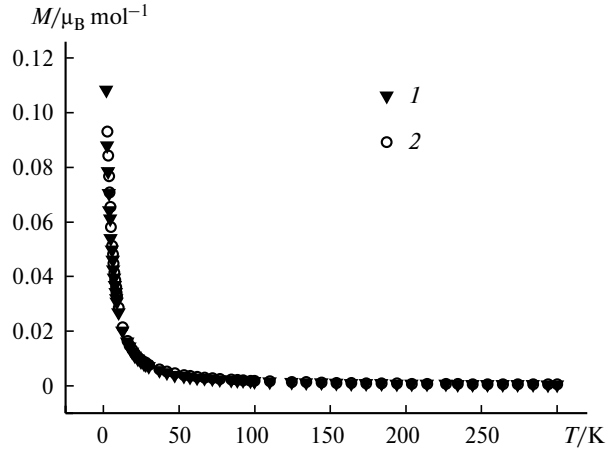

Fig. 12. Molar magnetic moment of complex **3** *vs.* temperature measured on zero-field cooling (*1*) and on field cooling at H = 100 Oe (*2*).

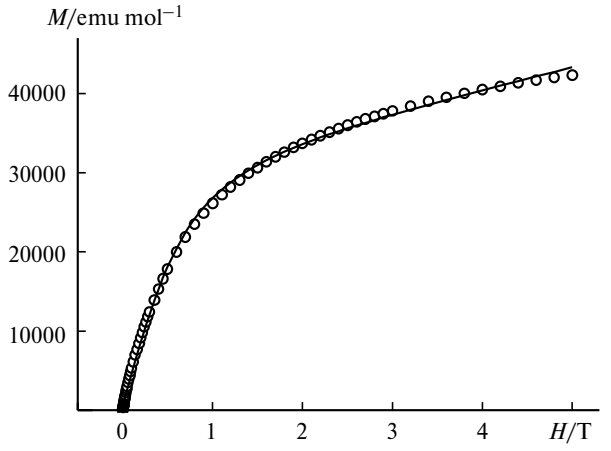

Fig. 13. Molar magnetic moment of sample **3** *vs.* external magnetic field measured at 2 K.

Analysis of the Fe^{57} Mössbauer spectroscopy data for sample **3** helped to clarify this point. The intermediate values of the isomer shifts of the two states of iron at room temperature (see Table 3) can be characterized as close to Fe^{2+} and Fe^{3+}; as the temperature decreases, they further approach the pure states. In addition, at T = 85 K, a component (~28%) with the isomer shift δ_{Fe} = = 0.72(2) mm s^{-1} typical of the $Fe^{2.5+}$ state with an intermediate charge appears in the spectrum. Presumably, the presence of several states of iron is due to the formation of Fe^{3+} and the triply charged $(C_6O_4Cl_2)^{\cdot 3-}$ radical anion upon the "extra"-dπ-electron transfer from some Fe^{2+} ions to the vacant π^* orbital of the non-magnetic bridging $(C_6O_4Cl_2)^{2-}$ ligand with similar energy. This is the known valence tautomerism (redox isomerism) phenomenon, which was observed, in particular, in binuclear iron complexes with anions of dihydroxybenzoquinone and its derivatives.[18,37] Moreover, according to Mössbauer data, the Fe^{2+} and Fe^{3+} states with unusual isomer shifts at room temperature appear as partially charge-delocalized states on the Mössbauer spectroscopy time scale of ~10^{-7} s. Thus, in complex **3**, the Fe^{2+} "extra"-dπ-electrons are delocalized (partly or completely, depending on the temperature) over all positions of the magnetically active sublattice.

These findings are not unusual or novel. For example, for symmetric mixed-valence complexes, $\{Fe^{3+}(d\alpha)^5/Fe^{2+}(d\alpha)^5(d\beta)\}$, direct overlap of the d-orbitals of the magnetic centers results in complete delocalization of the Fe^{2+} dβ electron between the two centers down to helium temperatures.[38,39] The Mössbauer spectra exhibit only one quadrupole doublet with the isomer shift corresponding to the formal iron oxidation state +2.5. However, in asymmetric binuclear complexes, the structural non-equivalence of the magnetic centers results in gradual localization of the Fe^{2+} and Fe^{3+} states on temperature decrease.[40]

It is obvious that in complex **3**, the delocalization of the Fe^{2+} "extra"-dπ electrons is not direct but occurs through vacant π* orbitals of the bridging $(C_6O_4Cl_2)^{2-}$ ligand.

Since the electron transfer is not accompanied by spin reversal, then in view of the Pauli exclusion, the spins of 3d ions in the M^{d+1}—L—M^d chain should be parallel. This is the so-called double exchange mechanism proposed[41] and later developed[42] to interpret the ferromagnetism and the metallic conductivity in mixed-valence manganites with the perovskite structure.[43] The concept of double exchange in the M^{d+1}—L—M^d chain is related to the "extra"-d-electron transfer to the ligand and simultaneous electron transfer from the ligand to the neighboring paramagnetic center as shown in Scheme 1. The double exchange parameter is normally several times as high as the superexchange interaction parameter of the localized electrons.[38]

Scheme 1

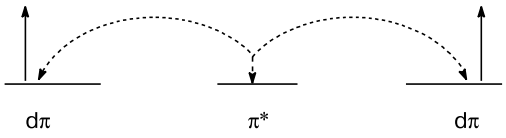

The assumption of mobility of the d electrons in complex **3** is supported by the measured electrical conductivity of the polycrystalline sample in the temperature range of 300—240 K (Fig. 14). The specific electrical conductivity of the polycrystalline sample at room temperature is $4 \cdot 10^{-5}\ \Omega^{-1}\ cm^{-1}$, which is five orders of magnitude greater than the electrical conductivity of metal complexes with localized charges. The dependence $\sigma(T)$ is of the semiconductor type. The activation barrier calculated from the Arrhenius equation is 0.16 eV.

In line with the foregoing, the existence of a radical oxygen species resulting from electron transfer from Fe^{2+} to the neighboring chloranilate leads to ferromagnetic correlation of the magnetic moments of iron ions. Note also that coupling of the localized moments Fe—$C_6O_4Cl_2^{\cdot 3-}$—Fe, like the double exchange related to extra-electron delocalization according to (Fe^{2+}—$C_6O_4Cl_2^{2-}$—Fe^{3+}) ↔ ↔ (Fe^{3+}—$C_6O_4Cl_2^{2-}$—Fe^{2+}) scheme, favors a parallel orientation of the iron spins. However, in the former case, the correlations should be antiferromagnetic due to the strong antiferromagnetic metal—radical coupling.[18,36,44]

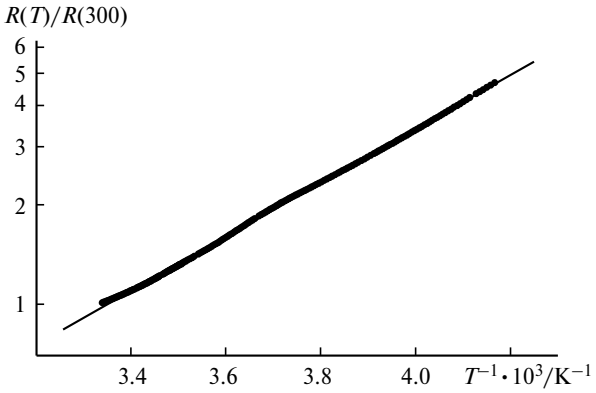

Fig. 14. Logarithm of the reduced electric resistance of sample **3** *vs.* reciprocal temperature. Linear extrapolation corresponds to the Arrhenius exponent with the activation energy of conduction $\Delta E = 0.16$ eV.

In the ideal case of ordered charge distribution in the network structure (see Fig. 5), one can distinguish zigzag-like one-dimensional Fe^{2+}—$C_6O_4Cl_2^{2-}$—Fe^{3+}—$C_6O_4Cl_2^{2-}$—... chains connected by $C_6O_4Cl_2^{3-}$ radical trianion bridges. The ferromagnetic coupling of iron moments within the chains according to the double exchange mechanism is stabilized by the Heisenberg Fe^{2+}—$C_6O_4Cl_2^{\cdot 3-}$—Fe^{3+} exchange between the chains. In this system, long-range ferro- or ferrimagnetic order with a high Curie temperature can be established.

In our system, which is disordered as regards the magnetic cations, chloranilate dianions, and radical trianions, exactly the iron valence state localization behavior on temperature decrease is observed. This can be clearly followed by looking at the temperature variation of the isomer shifts from Fe^{2+}- and Fe^{3+}-like states to nearly pure states (see Table 3) and the component corresponding to the mixed-valence $Fe^{2.5+}$ state, which is hardly detectable at room temperature. However, we cannot draw any conclusion about the mobility of the unpaired electron of the $C_6O_4Cl_2^{\cdot 3-}$ radical trianion. At low temperature, one should consider the case of nearly localized electrons, thus taking into account mainly the contribution of the superexchange interaction, M—$C_6O_4Cl_2^{2-}$—M and M—$C_6O_4Cl_2^{\cdot 3-}$—M, where M is any ion of the Fe^{2+}/Fe^{3+} pair. The absence of the transition to the magnetically ordered state at the lowest accessible temperature of 2 K also attests to disordered charge distribution and, as a consequence, to competition between ferro- and antiferromagnetic couplings with comparable magnitudes.

The obtained results open up the ways to the design and synthesis of a new class of metal complex bifunctional polymers that combine ferromagnetism and electron conduction within the same sublattice.

The authors are grateful to A. I. Dmitriev and F. V. Mushenok for the help in the magnetic measurements.

This work was supported by the Presidium of the Russian Academy of Sciences (Program No. 7 "Developments of the preparation methods of chemicals and the design of new materials", section "Polyfunctional materials for molecular electronics") and the Joint Grant of the Russian Foundation for Basic Research and CNRS (France) (Project No. 11-03-91054).

References

1. V. I. Ovcharenko, R. Z. Sagdeev, *Usp. Khim.*, 1999, **68**, 381 [*Russ. Chem. Rev.* (*Engl. Transl.*), 1999, **68**].
2. Z. J. Zhong, N. Matsumoto, H. Okawa, S. Kida, *Chem. Lett.*, 1990, 87.
3. H. Tamaki, M. Mitsumi, K. Nakamura, N. Matsumoto, S. Kida, H. Okawa, S. Ijima, *Chem. Lett.*, 1992, 1975.
4. H. Tamaki, Z .J. Zhong, N. Matsumoto, S. Kida, M. Koikawa, N. Achiva, Y. Nachimoto, H. Okawa, *J. Am. Chem. Soc.*, 1992, **114**, 6974.
5. L. O. Atovmyan, G. V. Shilov, R. N. Lyubovskaya, E. I. Zhilyaeva, N. S. Ovanesyan, S. I. Pirumova, I. G. Gusakovskaya, *Pis'ma v Zh. Eksp. Teor. Fiz.*, 1993, **58**, 818 [*JETP Lett.* (*Engl. Transl.*), 1993, **58**, 766].
6. C. Mathoniere, S. G. Carling, Y. Dou, P. Day, *Chem. Commun.*, 1994, 1551.
7. C. Mathoniere, C. J. Nutall, S. G. Carling, P. Day, *Inorg. Chem.*, 1996, **35**, 1201.
8. N. S. Ovanesyan, G. V. Shilov, L. O. Atovmyan, R. N. Lyubovskaya, A. A. Pyalling, *Mol. Cryst. Liq. Cryst.*, 1995, **273**, 175.
9. S. Decurtins, H. W. Schmalle, P. Schneuly, J. Ensling, P. Gutlich, *J. Am. Chem. Soc.*, 1994, **116**, 9521.
10. E. Coronado, J. R. Galan-Mascaros, C. G. Gomez-Garcia, E. Martinez-Ferrero, M. Almeida, *Eur. J. Inorg. Chem.*, 2005, 2064.
11. S. Benard, P. Yu, J. P. Audiere, E. Riviere, R. Clement, J. Guilhem, L. Tchertanov, K. Nakatani, *J. Am. Chem. Soc.*, 2000, **122**, 9444.
12. E. Coronado, J. R. Galan-Mascaros., C. J. Gomez-Garcia, V. Laukhin, *Nature (London)*, 2000, **408**, 447.
13. M. Gruselle, C. Train, K. Boubekeur, P. Gredin, N. S. Ovanesyan, *Coord. Chem. Rev.*, 2006, **250**, 2491.
14. S. M. Aldoshin, L. A. Nikonova, G. V. Shilov, E. A. Bikanina, N. K. Artemova, V. A. Smirnov, *Mol. Struct.*, 2006, **794**, 103.
15. C. G. Pierpont, L. C. Francesconi, D. H. Hendickson, *Inorg. Chem.*, 1977, **16**, 2367.
16. D. F. Xiang, C. Y. Duan, X. S. Tan, Y. J. Liu, W. X. Tang, *Polyhedron*, 1998, **17**, 2647.
17. M. Kawahara, M. K. Kabir, K. Yamada, K. Adachi, H. Kumagai, Y. Narumi, K. Kindo, S. Kitagawa, S. Kawata, *Inorg. Chem.*, 2004, **43**, 92.
18. A. Dei, D. Gatteschi, L. Pardi, U. Russo, *Inorg. Chem.*, 1991, **30**, 2589.
19. K. S. Min, A. G. DiPasquale, J. A. Golen, A. L. Rheingold, J. S. Miller, *J. Am. Chem. Soc.*, 2007, **129**, 2360.
20. J. T. Wrobleski, D. B. Brown, *Inorg. Chem.*, 1979, **18**, 498.
21. S. Kawata, S. Kitagawa, H. Kumagai, T. Ishiyama, K. Honda, H. Tobita, K. Adachi, M. Katada, *Chem. Mater.*, 1998, **10**, 3902.
22. B. F. Abrahams, K. D. Lu, B. Moubaraki, K. S. Murray, R. Robson, *J. Chem. Soc., Dalton Trans.*, 2000, 1793.
23. S. Kawata, S. Kitagawa, I. Furuchi, C. Kudo, H. Kamesaki, M. Kondo, M. Katada, M. Munakata, *Mol. Cryst. Liq. Cryst.*, 1995, **274**, 179.
24. S. Kawata, S. Kitagawa, M. Kondo, I. Furuchi, M. Munakata, *Angew. Chem., Int. Ed.*, 1994, **33**, 1759.
25. H. Kumagai, S. Kawata, S. Kitagawa, *Inorg. Chim. Acta*, 2002, **337**, 387.
26. M. K. Kabir, M. Kawahara, H. Kumagai, K. Adachi, S. Kawata, T. Ishii, S. Kitagawa, *Polyhedron*, 2001, **20**, 1417.
27. S. Kawata, S. Kitagawa, H. Kumagai, C. Kudo, H. Kamaesaki, T. Ishiyama, R. Suzuki, M. Kondo, M. Katada, *Inorg. Chem.*, 1996, **35**, 4449.
28. M. K. Kabir, S. Kawata, K. Adachi, H. Tobita. N. Miyazaki, H. Kumagai, M. Katada, S. Kitagawa, *Mol. Cryst. Liq. Cryst.*, 2000, **341**, 491.
29. K. Nagayoshi, M. D. Kabir, H. Tobita, K. Honga, M. Kawahara, M. Katada, K. Adachi, H. Nishikawa, I. Ikemoto, H. Kumagai, Y. Hosokoshi, K. Inoue, S. Kitagawa, S. Kawata, *J. Am. Chem. Soc.*, 2003, **125**, 221.
30. Tzuoo-Tsair Luo, Yen-Hsiang Liu, Hui-Lien Tsai, Chan-Cheng Su, Chuen-Her Ueng, Kuang-Lieh Lu, *Eur. J. Inorg. Chem.*, 2004, 4253.
31. P. E. Riley, S. F. Haddad, K. N. Raymond, *Inorg. Chem.*, 1983, **22**, 3090.
32. B. F. Abrahams, J. Coleiro, K. Ha, B. F. Hoskins, S. D. Orehard, R. Robson, *J. Chem. Soc., Dalton Trans.*, 2002, 1586.
33. Z. K. Nikitina, V. D. Makhaev, N. S. Ovanesyan, G. V. Shilov, S. M. Aldoshin, *Int. Conf. Organometallic and Coord Chem. (Russia, N. Novgorod, 2008, 2—8 September), Book of Abstracts*, N. Novgorod, 2008, 74.
34. Z. K. Nikitina, N. S. Ovanesyan, V. D. Makhaev, G. V. Shilov, S. M. Aldoshin, *Dokl. Akad. Nauk*, 2011, **437**, 778 [*Dokl. Chem.* (*Engl. Transl.*), 2011, **437**, Pt. 2, 129].
35. G. M. Sheldrick, *SHELXTL v. 6.14, Structure Determination Software Suite*, Bruker AXS, Madison, Wisconsin, USA, 2000.
36. K. P. Butin, E. K. Beloglazkina, N. V. Zyk, *Usp. Khim.*, 2005, **74**, 585 [*Russ. Chem. Rev.* (*Engl. Transl.*), 2005, **74**].
37. K. S. Min, A. L. Reingold, J. S. Miller, *J. Am. Chem. Soc.*, 2006, **128**, 40.
38. X.-Q. Ding, E. L. Bominar, E. Bill, H. Winkler, A. X. Trautwein, S. Drueke, P. Chaudhuri, K. Wieghardt, *J. Chem. Phys.*, 1990, **92**, 178.
39. D. Lee, C. Krebs, B. H. Huynh, M. P. Hendrich, S. J. Lippard, *J. Am. Chem. Soc.*, 2000, **122**, 5000.
40. X.-Q. Ding, E. Bill, A. X. Trautwein, H. Winkler, A. Kostikas, V. Papaefthymiou, A. Simopoulos, P. Beardwood, J. F. Gibson, *Chem. Phys.*, 1993, **99**, 6421.
41. C. Zener, *Phys. Rev.*, 1951, **81**, 403.
42. P. W. Anderson, H. Hasegawa, *Phys. Rev.*, 1955, **100**, 675.
43. G. H. Jonker, J. H. Van Santen, *Physica*, 1950, **16**, 599.
44. J. S. Miller, K. S. Min, *Angew. Chem., Int. Ed.*, 2008, **47**, 2.

Received March 4, 2011;
in revised form April 8, 2011